COBEM 2023 27TH INTERNATIONAL CONGRESS OF MECHANICAL ENGENEERING

ABCM Brazilian Society of Mechanical Sciences and Engineering
27th ABCM International Congress of Mechanical Engineering
December 04-08, 2023, Florianópolis-SC, Brazil

COB-2023-0426 APPLICATION OF GITT FOR THE CHARACTERIZATION OF THE THERMAL BOUNDARY LAYER USING A NON-INVASIVE METHOD WITH A CAPACITIVE SENSOR

F.A. LIMA [1]
F.A. BELO [2]
[1] Instituto Federal da Paraíba, Jd Oásis, Cajazeiras - PB - Brasil - CEP:58900-000
[2] Universidade Federal da Paraíba, Cidade Universitária - João Pessoa - PB - Brasil - CEP: 58051-900
fabio.lima@ifpb.edu.br, franciscoantoniobelo@gmail.com
D.L.A. VELOSO [3]
[3] Instituto Federal da Paraíba, Jaguaribe, João Pessoa - PB - Brasil - CEP:58015-430
dhiego_vel@hotmail.com
G.E. ASSAD [4]
[4] Instituto Federal da Paraíba, Santa Rita - PB - Brasil - CEP: 58.301-645
gustavo.assad@ifpb.edu.br
I.C. SILVEIRA [5]
[5] Instituto Federal de Pernambuco - Campus Caruaru PE Estrada do Alto do Moura, KM 3,8, s/n - Distrito Industrial III, Caruaru - PE, 55040-120
igor.silveira@caruaru.ifpe.edu.br
A.G.A. GIUSEPPE[6]
[6] Instituto Federal da Paraíba - Campus Itaporanga PB 386, Km 2 - CEP: 58.780-000. - Itaporanga/PB
allan.caldas@ifpb.edu.br

Abstract. *The thermal boundary layer corresponds to a variation in the temperature field, which occurs in a narrow region close to the wall of a solid body, when it is exposed to a flow of a fluid at a temperature different from its own. Its study is important in the design of cooling systems for electrical and electronic components and in capturing solar energy. For the study of the thermal boundary layer, authors have presented invasive measurement methods. The present work intends to present a characterization of the thermal boundary layer based on a non-invasive method based on the electromagnetic field model of a capacitive sensor. The liquid that fills the inside of a tube in a circular shape together with a borosilicate glass tube, becomes the dielectric of the capacitor constituted by the plates, making the sensor response variable according to the characteristics of the liquid that is present inside it. . The modeling will be performed using the Generalized Integral Transform Technique (GITT), the velocity profile will be considered fully developed at the thermal input, the effects of viscous dissipation will not be considered, and the axial diffusion of the fluid along the flow will be neglected.*
Keywords: thermal boundary layer, GITT, Capacitive Sensor

1. INTRODUCTION

According to Dewitt (2008) the boundary layer concept is crucial for understanding convective heat and mass transfers between a surface and a flowing fluid in contact with this surface. Dewitt (2008) also states that the boundary layers may be of velocity, thermal and concentration types.
In a solid body exposed to the flow of a fluid at a temperature different from its own, the variation in the temperature field will occur in a narrow region near the wall, similar to the velocity field. This region, in analogy with the dynamic process, is usually called the thermal boundary layer (Pantaleão, 1990).

Study of thermal boundary layers is important for several industrial applications, such as cooling system design for electronic components, solar energy capture, geothermal reservoirs, advanced oil recovery and cooling of nuclear reactors, among others (Makinde, 2012). The characterization of the thermal boundary layer is a limiting factor in several applications because if the temperature distribution in the thermal boundary layer is known, it is possible to directly calculate the heat transfer from a solid surface (Kulkarni, 2011).

Even though many important applications have been presented, the best-known methods for thermal boundary layer characterization, either in ducts or plates, are usually invasive, i.e., there is contact between the sensor and the liquid, which directly interferes with its flow (Slangen, 2009; Puttkammer, 2013; Carey, 1978; Bhattacharyya, 2016 and Bellec, 2016); usually, the sensors used for this purpose are thermocouples and hot wire anemometers.

Thermal boundary layers are also studied in (Han, 2007 and Farzad, 2014) with intrusive (invasive) analysis methods using thermocouples or TDRs (Temperature Detection Resistors); these studies perform dynamic analyses of the fluid. Feng Xu (2009) presents a static analysis of the thermal boundary layer; however, they do not present any results related to the verification of the layer's thickness.

As an attempt to probe the thermal boundary layer via non-invasive means, J.L. Xu et al. (2005) used infrared analysis, but the final focus of these studies was the analysis of the local Nusselt number's behavior.

In Rahim, (2018), the numerical algorithm NAG (Numerical Algorithms Group) was used to verify the laminar flow of the thermal boundary layer in rotating spheres. Suvash et al., (2014), performed a numerical investigation in which the fluid used was air. D. Andrew (2015), performed a theoretical study of a Bingham fluid in a porous medium, and Mart, (2011), developed an experimental study of the turbulent thermal boundary layer on a flat plate.

Theoretical characterizations of thermal boundary layers were also performed by (Makinde, 2012; Mart, (2011); Thomas, (1978) and Martin Schmitt, (2015)), using mathematical methods such as Runge-Kutta-Fehlberg, the integral energy equation, and DNS (direct numerical simulation), and those studies analyzed variations in the Prandtl or Nusselt numbers in the thermal boundary layers.

For the theoretical analysis of thermal boundary layers, the present work proposes a numerical method, the GITT (generalized integral transform technique), that has been used with satisfactory results. The GITT is presented in Ghiaasiaan, (2011), as a theoretical solution, in which heat transfer in the axial direction is ignored and Hagen-Poiseuille is applied to the thermal boundary layer problem, whereas Silva, (2016) considers the axial direction and uses the GITT for mathematical modeling. In this work, we will use the method proposed in Silva, (2016).

The aim of this work is to present a new method for characterizing thermal boundary layers in a non-invasive manner, i.e., without interfering with the flow of the fluid to be analyzed. For this purpose, a mixture analyzer composed of circular 316-L stainless-steel tubes with 10 mm external diameter and 8 mm internal diameter, thermistors, thermocouples and a capacitive type sensor will be used. This sensor consists of two semi-cylindrical copper plates in opposite positions of a borosilicate glass tube. The liquid that fills the interior of the tube and the borosilicate glass tube serves as the dielectric of the capacitor constituted by the plates, making the sensor's response vary according to the characteristics of the liquid that is present inside the tube. The model of the sensor that will perform the characterization of the thermal boundary layer is set up as in Belo, (1982), where it is used to perform concentration measurements in a water/alcohol mixture. The modeling of the thermal problem, necessary to understand the problem and obtain the theoretical results, is performed using the GITT.

2. PHYSICAL PROBLEM

The physical problem consists of the flow of a Newtonian fluid (in our study, distilled water) in the thermal inlet region of a circular duct, as shown in Figure 1.

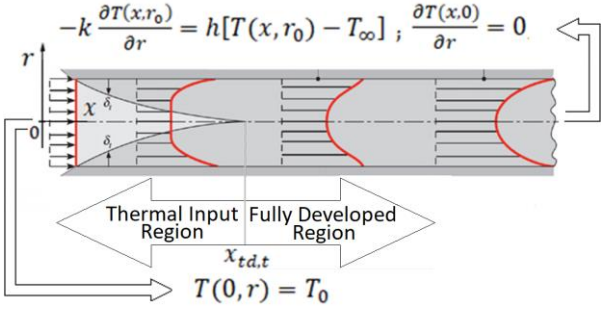

Fig. 1. Illustration of the physical problem [26].

Considering that the flow regime is laminar and permanent and that the fluid is incompressible with constant thermophysical properties, one can write the energy equation and the boundary and inlet conditions for the cylindrical coordinate system as follows:

Energy Equation:

$$\rho c_p u(r)\frac{\partial T(x,r)}{\partial x} = k\left[\frac{1}{r}\frac{\partial}{\partial r}\left(r\frac{\partial T(x,r)}{\partial r}\right)\right];\ 0 < r < r_0,\quad x > 0 \tag{1a}$$

Boundary conditions:

$$\frac{\partial T(x,r)}{\partial r} = 0, \quad r = 0, \ x > 0 \tag{1b}$$

$$k\frac{\partial T(x,r)}{\partial r} + h[T(x,r) - T_\infty] = 0, \ r = r_0, \ x > 0 \tag{1c}$$

Inlet condition:

$$T(x,r) = T_0, \quad x = 0 \tag{1d}$$

where r represents the radius of the tube and ρ, c_p and k represent the fluid's density, specific heat at constant pressure and thermal conductivity, respectively. The fully developed laminar flow velocity profile is represented by $u(r)$.
In the present work, the velocity profile is fully developed at the thermal inlet (Kakaç, (1995) and Lipkis, (1954)), the effects of viscous dissipation will not be considered; impermeability and no-slip conditions at the walls will be assumed; body forces will be ignored; no internal energy generation will be assumed, and the axial diffusion of the fluid throughout the flow will also be ignored

3. DIMENSIONLESS OF THE PROBLEM FOR APPLICATION OF THE GITT

To solve the family of problems that are defined by the proposed model, the parameters and dimensionless groups presented in Ghiaasiaan, (2011) and Mikhailov, (1983) will be used:

$$R = \frac{r}{r_0} \tag{2a}$$

$$\xi = \frac{2x}{D_h Re_d Pr} \tag{2b}$$

$$\theta(\xi, R) = \frac{T(x,r) - T_\infty}{T_0 - T_\infty} \tag{2c}$$

$$U(R) = \frac{u(r)}{u_m} \tag{2d}$$

where R is the dimensionless radius; T_∞ and T_0 represent the ambient temperature and the fluid inlet temperature, respectively; Bi, Re_D and Pr are dimensionless numbers called the Biot number, Reynolds number and Prandlt number, respectively, whose definitions are as follows:

$$Bi = \frac{hr_0}{k} \tag{2e}$$

$$Re_D = \frac{u_m D_h}{\nu} \tag{2f}$$

$$Pr = \frac{\nu}{\alpha} \tag{2g}$$

with u_m representing the average flow velocity, r_0 the radius of the circular tube, $D_h = 2r_0$ the tube hydraulic diameter, ν the kinematic viscosity of the fluid, and $\alpha = \frac{k}{\rho c_p}$ the thermal diffusivity of the fluid.

Dimensionless energy equation:

$$U(R)\frac{\partial \theta(\xi,R)}{\partial \xi} = \frac{2}{R}\frac{\partial}{\partial R}\left[R\frac{\partial \theta(\xi,R)}{\partial R}\right]; O < R < 1, \xi > O \tag{3a}$$

Dimensionless boundary conditions:

$$\left.\frac{\partial \theta(\xi,R)}{\partial R}\right|_{R=0} = O \ , R = O \ ; \xi > O \tag{3b}$$

$$\frac{\partial \theta(\xi,R)}{\partial R} + Bi\ \theta(\xi,R) = O \qquad R = 1 \ , \quad \xi > O \tag{3c}$$

Dimensionless inlet condition:

$$\theta(\xi, R) = 1\,; \xi = 0, \quad O \leq R \leq 1 \tag{3d}$$

The dimensionless velocity profile used is

$$U(R) = \ 2[1 - R^2] \tag{4}$$

3.1 Generalized Integral Transform Technique

To solve problems using the GITT, a few steps are needed. The first of them is to define an auxiliary problem to determine the temperature field:

$$\frac{d}{dR}\left(R\,\frac{d\psi_i(\mu_i,R)}{dR}\right) + \mu_i^2 R\ U(R)\psi_i(\mu_i, R) = O,\ 0 < R < 1 \tag{5a}$$

$$\frac{\partial\psi_i(\mu_i,R)}{\partial R} = O,\ \ R = O,\ \ \mu_i > 0 \tag{5b}$$

$$\frac{\partial\psi_i(\mu_i,R)}{\partial R} + \mathrm{Bi}\psi_i(\mu_i, \mathrm{R}) = 0,\ \ \mathrm{R} = 1,\ \ \mu_i > 0 \tag{5c}$$

To solve this type of problem, Mikhailov (1983), proposed the method of signal counting. This method allows calculating the eigenvalues, the eigenfunctions and the norms, without loss of information in the application of the methodology (Cotta, (1993)).

3.2 Determination of the Inverse-Transform pair

The second step is to define an inverse-transform pair to represent the problem:

$$\overline{\theta}_i(\xi) = \frac{1}{N_i^{1/2}} \int_0^1 \mathrm{R}\,\mathrm{U}(\mathrm{R})\psi_i(\mu_i, \mathrm{R})\theta(\xi, \mathrm{R})\mathrm{dR}\ , \text{ Transform} \tag{6a}$$

$$\theta(\xi, \mathrm{R}) = \ \sum_{i=1}^{\infty} \frac{1}{N_i^{1/2}} \psi_i(\mu_i, \mathrm{R})\,\overline{\theta}_i(\xi)\ , \text{ Inverse} \tag{6b}$$

The third is to apply the transform definition given by equation (6a) and to use the auxiliary problem defined by (5a), thus transforming the dimensioless energy equation (3a) into a system of ordinary differential equations (ODEs), as in Equation (7).

$$\frac{1}{2}\frac{d\overline{\theta}_i(\xi)}{d\xi} + \mu_i^2\overline{\theta}_i(\xi) = 0 \tag{7}$$

The fourth step is to solve the obtained system; in this case, this system has the following classic analytical solution:

$$\overline{\theta}_i(\xi) = \ \bar{f}_i\ \ e^{-2\mu_i^2\,\xi} \tag{8}$$

such that $\overline{f}_i = \frac{B_i\psi_i(\mu_i,1)}{N_i^{1/2}\mu_i^2}$

Finally, the temperature field for the thermal inlet region takes the following form:

$$\theta_i\left(\xi, R\right) = \sum_{i=0}^{\infty} \frac{\psi_i(\mu_i, R).\,\bar{f}_i.e^{-2\mu_i^2\xi}}{N_i^{1/2}} \tag{9}$$

The dimensionless average temperature can be calculated using the following expression:

$$\theta(\xi)_{average}=\frac{\int_0^1 \mathrm{RU(R)}\theta(\xi,\mathrm{R})\mathrm{dR}}{\int_0^1 \mathrm{RU(R)dR}} \tag{10a}$$

After mathematical manipulations, it can be shown that

$$\theta(\xi)_{average} = 2.\sum_{i=0}^{\infty} \bar{f}_i^{\,2}.e^{-2\mu_i^2\xi} \tag{10b}$$

4. MIXTURE ANALYZER BY DIPOLE POLARIZATION

The Mixture Analyzer by Dipole Polarization (MADP) was developed by Silva, (2016). The MADP is based on the degree of dipole polarization of the matter at different electronic frequencies and at a certain temperature. For dipole mixtures, the dipole polarization is determined by the electrical permittivity, the electronic frequency of the electrodes (the mixture is between them) and the temperature of the sample. The developed equipment accurately measures temperature values and mixture polarization under static and dynamic conditions and, using calibration correlations, transforms them into concentration values.

Validation of the polarization for analysis of the mixture in a static regime or for the laboratory has been studied since the beginning of the 1980s. The first patent application was presented in Belo, (1982), and presented at fairs (II FEBRAN, Belo, (2002)) and at SINST-PADCT, Belo (1988). It was presented in SAE, Belo (1982), with an accuracy suitable for laboratory analysis of ethanol and at the International Oil Fair, Belo, (1993). High precision and robustness were obtained only in 2009 with anembedded electronics, Belo, (2009), and the method was applied to various biofuels and transformer oil, with an accuracy on the order of PPM (parts per million).

4.1 Capacitive Sensor

When a molecule has a dipole, it is called a polar molecule. For a molecule to have a dipole, there are two criteria. First, it must have polar bonds. Second, the dipoles created by these bonds should not vanish as a result of the symmetry created in the molecule. In most capacitors, there is an insulating material, such as paper or plastic, between their plates. Such a material that can be used to maintain the physical separation between the plates is called dielectric Belo, (2015) and Gonçalves, (2015). Dielectric materials consist of many permanent or induced dipoles. One of the fundamental concepts for understanding dielectrics is the average electric field produced by a large number of aligned small electrical dipoles. With this principle, the Research Group on Instrumentation and Control and on Energy and Environmental Study (Grupo de Pesquisa em Instrumentação e Controle e em Estudo de energia e Meio Ambiente - GPICEEMA) developed the capacitive sensor used in this work. It is comprised of two semi-cylindrical copper plates in opposite positions of a borosilicate glass tube, as shown in Figure 2.

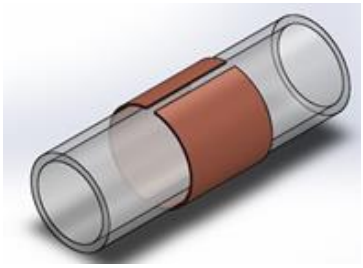

Fig. 2. Capacitive Sensor, Gonçalves, (2015).

During polarization, the charges bound to the molecules are subject to displacement, but without leaving the boundaries of the molecules (as opposed to electrical conduction). Polarization occurs in all molecules of the dielectric, being a property of its whole volume. Each material has a characteristic polarization. Each dipole liquid has a characteristic polarization for the same external field, which varies with the thermal field (temperature field) within it. Different dipole materials have different polarizations for the same corresponding thermal fields.

Water is one of the materials that has the largest variation in polarization and therefore permissiveness with temperature, Fink, (1982). Samples of water at different temperatures behave as different dipole materials, i.e., respond

as different materials to an external field. This behavior allows applying the annular flow model, according to Belo, (1995) and Belo, (1999).

The resolution of the measurement of the thermal boundary layer's length variation is determined by the length of the electrodes. To obtain the radius of the wall corresponding to the width of the flow's thermal layer, these elements must be related to the equation of the electric field. Considering the geometry of the sensor, the electrodes are external to the insulation material. In this manner, one can consider that the electric fields due to the potentials of the electrodes will propagate in three materials: the glass, the boundary layer and the region exterior to the boundary layer.

Figure 3 is intended to show some visual representations at two cross-sectional positions of the flow sensor (which is represented by the electrodes), flow duct, flow wall or internal radius of the duct and radius of the boundary layer. This is its application, which is generally called a non-invasive and non-intrusive cell. In (a) and (b), the green regions are of the glass tube. The darker regions of (a) and (b) correspond to the thicknesses of the boundary layer at positions closest to and furthest from the inlet, respectively. In (b), there is R_2, the radius of the flow wall, or the internal radius of the glass. The central regions of (a) and (b) correspond to regions outside the boundary layer. In (c), the electrodes are positioned at generic positions with the electrode angles given by θ_1, θ_2, θ_3 and θ_4. ε_1, ε_2 and ε_3 are the electrical permitivities of the corresponding materials.

$\varepsilon_1 \rightarrow$ Relative permitivity outside the boundary layer;
$\varepsilon_2 \rightarrow$ Relative permitivity within the boundary layer;
$\varepsilon_3 \rightarrow$ Relative Permissiveness of Glass

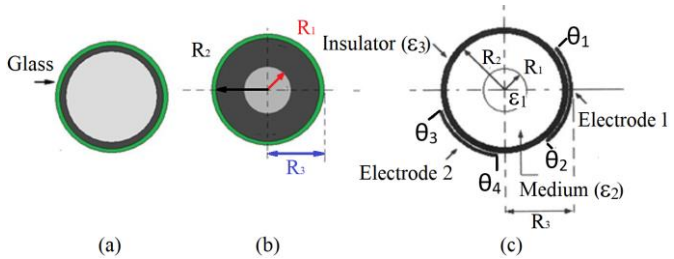

Fig. 3. Cross-sectional representation of the flow sensor and its polarization, flow and electric elements.

The solution to this problem applied to the flow corresponds to determining the impedance of the two electrodes at a generic angle external to the cylindrical duct. Belo, (1982), proposed and developed a model of the sensor, which is given by

$$\text{Cap} = \frac{2\,\varepsilon_0\varepsilon_2}{\pi}\left\{\ln\left[\frac{\sin\left(\frac{\theta_1+\theta_2}{2}\right)}{\sin\left(\frac{\theta_1-\theta_2}{2}\right)}\right] - \sum_{1}^{\infty}\frac{4(\text{ACF}_1^n + \text{BD})\,\sin(n\theta_1)\,\text{sen}(n\theta_2)}{n(\text{CDF}_2^n + \text{ABF}_3^n + \text{ACF}_1^n + \text{BD})}\right\} \tag{11}$$

where

$$A = \varepsilon_1 + \varepsilon_2$$
$$B = \varepsilon_2 + \varepsilon_3$$
$$C = \varepsilon_3 - \varepsilon_2$$
$$D = \varepsilon_2 - \varepsilon_1$$

$$F_1 = \left(\frac{R_2}{R_1}\right)^2, \qquad F_2 = \left(\frac{R_3}{R_2}\right)^2, \qquad F_3 = \left(\frac{R_3}{R_1}\right)^2$$

5. RESULTS

The characterization of the thermal boundary layer will be performed by measuring the properties of the liquid in the capacitive sensor, since the response of the sensor varies according to the properties of the liquid inside; when there is a thermal boundary layer, there will be the same liquid, but with different properties according to the existing temperature gradient. Thus, the response of the sensor can be used to characterize the thermal boundary layer based on the properties of the liquid at a given temperature; therefore, the response of the sensor will correspond to the liquid at the known

temperature and the same liquid at another temperature, that is, the capacitive sensor will identify two distinct liquids inside, since although they are the same liquid, their dielectric constants will be distinct due to their different temperatures.

According to Dewitt, (2008), far from the surface of the tube, the temperature profile is uniform T(y) = T∞; however, as the particles of the fluid come into contact with the surface of the tube, they come to a thermal equilibrium with the surface and temperature gradients develop. The region of the fluid in which these temperature gradients exist is the thermal boundary layer, and its thickness δt is typically defined as the value of y at which the ratio

$$\theta = \frac{T - T_S}{T_\infty - T_S} = 0.9 \tag{12}$$

Considering Equation (14) for surface temperatures of 296 and 293 K at the wall of the tube and volumetric flow rates of 8.3 × 10^{-6}, 16.67 × 10^{-6} and 27.33 × 10^{-6} m^3/s, data acquisition was performed, which can be observed in the graphs of Figures 4 a-c.

Since the value specified at the wall is 293 K, according to the calculations presented by Dewitt, (2008), it is concluded that the fully developed thermal boundary layer occurs when the liquid inside the tube has the temperature of 293.3 K over the whole radial extension.

For the purpose of analysis, the longitudinal distance (x-axis) of 1 meter in the circular tube was considered as a reference, where it is possible to verify in Figures 4 a-c that the smaller the volumetric flow rate, the faster the development of the temperature field and consequently of the thickness of the thermal boundary layer (y-axis).

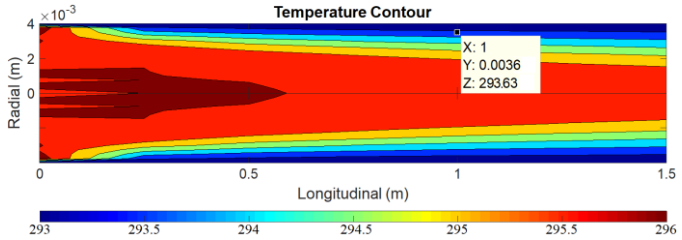

Fig. 4a. Thermal boundary layer at the duct's 1-meter position and the position where it becomes fully developed for a volumetric flow rate of 8.33 × 10-6 m3/s

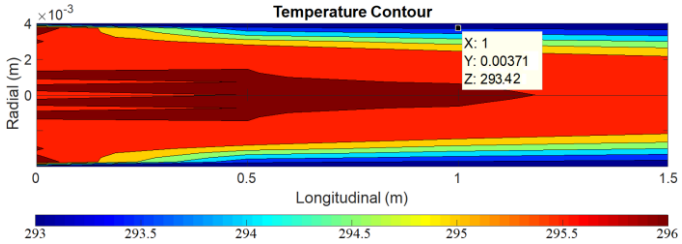

Fig. 4b. Thermal boundary layer at the duct's 1-meter position and the position where it becomes fully developed for a volumetric flow rate of 16.67 × 10-6 m3/s

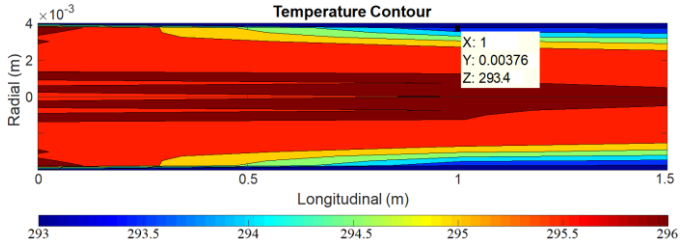

Fig. 4c. Thermal boundary layer at the duct's 1-meter position and the position where it becomes fully developed for a volumetric flow rate of 27.33 × 10-6 m3/s

5.1 Verification of the Theoretical Model Using the Capacitive Sensor Installed in the Mixture Analyzer

With the intent to correlate the capacitive sensor's response with the liquid's temperature, it becomes necessary to investigate this very possibility. To verify the feasibility of this approach, the calibration of the capacitive sensor was performed as a function of the temperature of the liquid (distilled water) inside. The result of this calibration is shown in Figure 5, where it is possible to observe its linearity, which means that the capacitive sensor is able to measure the temperature of the distilled water in a non-invasive manner in a static and dynamic form, that is, with and without fluid flow.

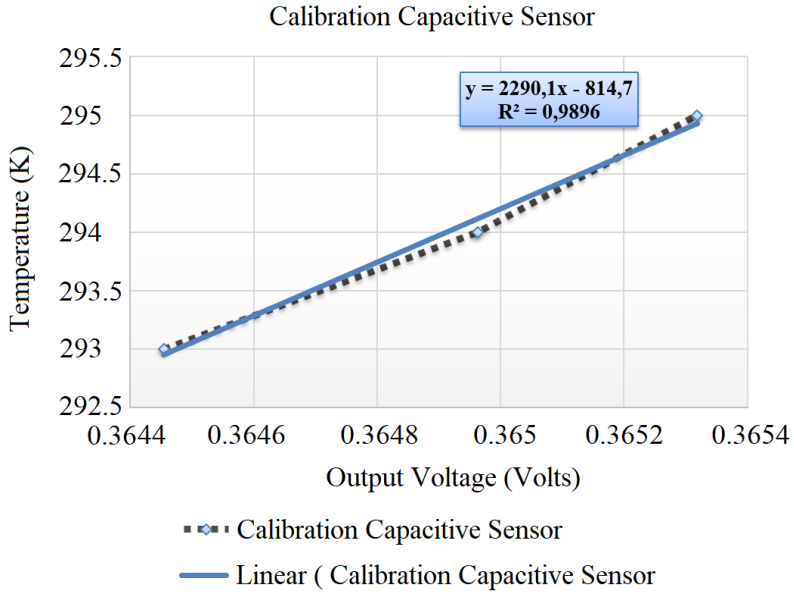

Figure 5. Capacitive Sensor Response to Distilled Water

The direct comparative analysis of the capacitive sensor responses for all volumetric flow rates and temperatures is shown in Figure 6. It is estimated that the fluid is fully developed, thermally and hydrodynamically; thus, the temperature must be homogeneous and with laminar flow only as soon as the temperature stabilizes. It is again found that the response of the capacitive sensor gives an estimate for the thickness of the thermal boundary layer when correlating the graph of Figure 7 with the results shown in Figures 4 a-c for the GITT model.

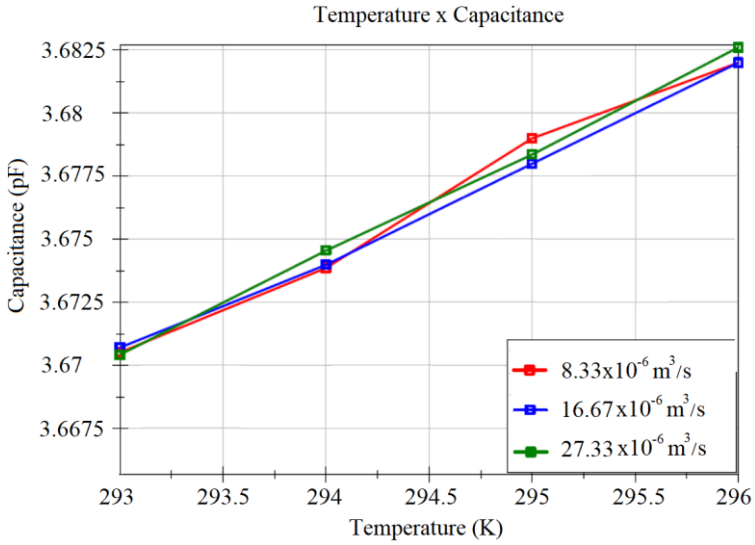

Figure 6. Capacitive Sensor Response for Distilled Water

Figure 7 shows in detail the thickness measurements obtained with the correlation between the values presented by the capacitive sensor and the GITT model for a temperature of 293 K at the tube's wall, 296 K at the surface and a volumetric flow rate of 8.3×10^{-6} m^3/s.

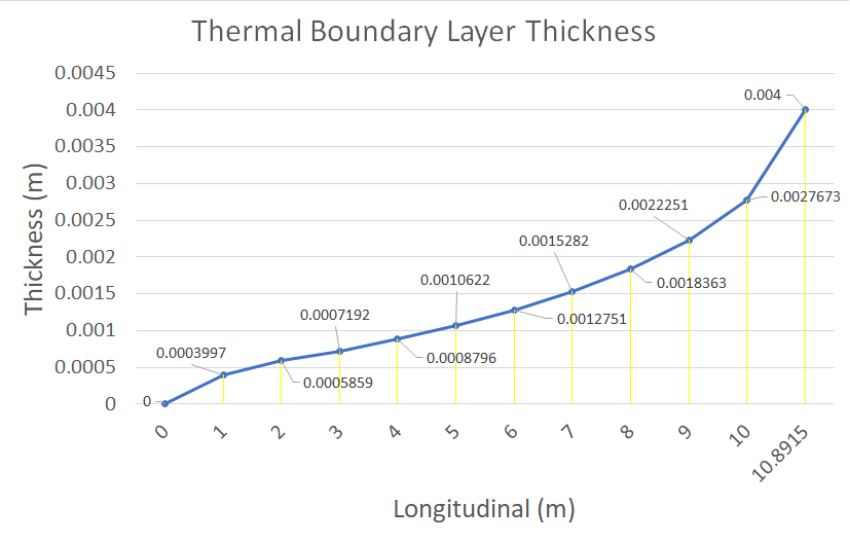

Figure 7. Thermal boundary layer thickness versus longitudinal position for an inlet temperature of 296 K

6. CONCLUSIONS

This paper presents a new method for the characterization of the thermal laminar boundary layer in circular ducts using a capacitive sensor, and its non-invasive nature is the main difference from the methods already presented in the literature.

The obtained results show that the GITT is an effective alternative for the resolution of the theoretical physical problem, and as an outcome, the smaller the flow rate, the slower the temperature field development and the slower the thermal boundary layer development.

One of the main difficulties encountered in the analysis is the effective control of the liquid's temperature in the flow, which directly influences the verification of the thermal boundary layer. The linear characteristics of the behavior of the capacitive sensor allow for a better point characterization of the thermal boundary layer.

It is concluded that the system achieved the proposed aims by comparing the results presented for the temperature field with the GITT model and the capacitance response shown in the sensor readings, where through a relation between the obtained values, it was possible to verify the thickness of the thermal boundary layer.

It is important to note that the proposed technique has never been used before, with this being the first example of an analysis of the thermal laminar boundary layer in circular ducts using a non-invasive method.

7. REFERENCES

BELLEC, M.; TOUTANT, A.; OLALDE, G. Large Eddy Simulations of thermal boundary layer developments in a turbulent channel flow under asymmetrical heating. Computers & Fluids, v. 151, p. 159–176, 2016.

BELO, F. A. Aplicação da Análise Eletrônica ao Estudo do Escoamento Multifásico, Tese de Doutorado, Programa de Pós-graduação em Engenharia Mecânica, UNICAMP, 1995.

BELO, F. A., "Etilômetro Eletrônico", Seminário de Instrumentação e Feira de Exposição de Protótipos, SINST/PADCT/CNPQ, USP, São Paulo, Brasil, 1988.

BELO, F. A., "Protótipo do Analisador de Mistura pela Polarização Dipolar", Apresentação na Feira Mundial Rio Oil & Gas, Rio de Janeiro, Brasil, 2002.

BELO, F. A., LIMA FILHO, A. C., DE BRITO, D. M. G., "Instrumento de Transdução Eletrônica Resistiva Múltipla com Compensação da Deriva Térmica e Ruído de Baixa Frequencia." Patente: Privilégio de Inovação. Número do registro: PI09027483, data de depósito: 30/07/2009. Instituição(ões) financiadora(s): Universidade Federal da Paraíba, Brasil, 2009.

BELO, F. A.; LIMA FILHO, A. C.; SILVA, F. A.; SILVA, T. A. B., "Analisador Eletrônico De Componentes De Mistura Pela Polarização Dipolar Para Laboratório E Controle De Processos" Patente Requerida, 2015.

BELO, F. A.; Medidor De Concentração Eletrônico; 1982, Brasil; Patente: Privilégio de Invenção, Número do registro: PI8207690, Instituição de registro: INPI - Instituto Nacional da Propriedade Industrial. Instituições financiadora(s): CNPQ e UFPB.

BELO, F. A.; MOURA, L. F. M. A High Frequency Electronic Transducer for Multiphase Flow Measurements; J. Brazilian Society Mechanical Sciences. Journal of the Brazilian Society of Mechanical Sciences and Engineering, Rio de Janeiro, v. 21, n. 4, p. 611-621, 1999.

BELO, F. A.; LEITE, J. T. F.; "Electronic analyser of quality". SAE Data Book, São Paulo, Brasil, 1993.

BHATTACHARYYA, K.; UDDIN, M. S.; LAYEK, G. C. Exact solution for thermal boundary layer in Casson fluid flow over permeable shrinking sheet with variable wall temperature and thermal radiation. Alexandria Engineering Journal, v. 55, n. 2, p. 1703–1712, 2016.

CAREY, V. P.; MOLLENDORF, J. C. Measured variation of thermal boundary-layer thickness with prandtl number for laminar natural convection from a vertical uniform-heat-flux surface. International Journal of Heat and Mass Transfer, v. 21, n. 4, p. 481–488, 1978.

COTTA, R. Integral Transform in Computational Heat and Fluid Flows. 1ª Edição ed. Flórida: CRC Press, Inc., 1993.

D. Andrew S. Rees, Andrew P. Bassom. Unsteady thermal boundary layer flows of a Bingham fluid in a porous medium. International Journal of Heat and Mass Transfer, v. 82, p. 460-467, 2015.

DEWITT, D. P. et al. Fundamentos de Transferência de Calor e Massa. 6ª ed. Rio de Janeiro - RJ: LTC, 2008.

FARZAD Houshmand, Yoav Peles. Heat transfer enhancement with liquid–gas flow in microchannels and the effect of thermal boundary layer. International Journal of Heat and Mass Transfer, v. 70, p.725-733, 2014.

FENG Xu, John C. Patterson, Chengwang Lei. Heat transfer through coupled thermal boundary layers induced by a suddenly generated temperature difference. International Journal of Heat and Mass Transfer, v. 52, p. 4966-4975, 2009.

FINK, D. G. (Editor in Chief) and Christiasen, D. (Associate Editor). Eletronics Enginers' Handbook, McGraw-Hill Book Company, 1982.

GHIAASIAAN, S. M. Convective Heat and Mass Transfer. 1ª ed. Los Angeles: Cambridge University Press, 2011.

GONÇALVES, P. G. Estudo Teórico e Experimental de um Analisador de Misturas pela Polarização Dipolar, Dissertação de Mestrado, UFPB, João Pessoa, 2015.

HAN, S.; Goldstein, R. J. Heat Transfer Study in a Linear Turbine Cascade Using a Thermal Boundary Layer Measurement Technique. Journal of Heat Transfer, v. 129, n. 10, p. 1384-1394, 2007

J.L. Xu, Y.H. Gan, D.C. Zhang, X.H. Li. Microscale heat transfer enhancement using thermal boundary layer redeveloping concept. International Journal of Heat and Mass Transfer, v. 48, p. 1662-1674, 2005.

KAKAÇ, S. and YENER, Y., Convective Heat Transfer, CRC Press, Inc., Florida, EUA, 1995.

KULKARNI, K. S.; HAN, S.; GOLDSTEIN, R. J. Numerical simulation of thermal boundary layer profile measurement. Heat and Mass Transfer, v. 47, n. 8, p. 869–877, 2011.

LIPKIS,R.P., Heat Transfer to an Incompressilble Fluid in Laminar Motion, M.Sc. Thesis, University of California, Los Angeles, 1954.

MAKINDE, O. D. Effect of variable viscosity on thermal boundary layer over a permeable flat plate with radiation and a convective surface boundary condition. Journal of Mechanical Science and Technology, v. 26, n. 5, p. 1615–1622, 2012.

MART, Steven R.; McClain, Stephen T. Protuberances in a Turbulent Thermal Boundary Layer. Journal of Heat Transfer. v. 134, p. 011902-011902-12, 2011.

MARTIN Schmitt, Christos E. Frouzakis, Yuri M. Wright, Ananias G. Tomboulides, Konstantinos Boulouchos. Direct numerical simulation of the compression stroke under engine-relevant conditions: Evolution of the velocity and thermal boundary layers, International Journal of Heat and Mass Transfer, v. 91, p. 948-960, 2015.

MIKHAILOV, M. D.; and VULCHANOV, N. L.; "Computational procedure for Sturm-Liouville problems", Journal of computational Physics, v. 5, 323-336, 1983.

PANTALEÃO, A.; FREIRE, S. Teoria de Camada Limite.Disponível:<http://www.turbulencia.coppe.ufrj.br/notas_aulas/CursoCamadaLimite_APSF.pdf>, Rio de Janeiro, 1990.

PUTTKAMMER, P. P. Boundary layer over a flat plate. BSc Report, v. 17, n. June, p. 331–355, 2013.

RAHIM Shah, Tongxing Li. The thermal and laminar boundary layer flow over prolate and oblate spheroids. International Journal of Heat and Mass Transfer, v. 121, p. 607-619, 2018.

SILVA, J. F. Método não invasivo de determinação da camada limite térmica em escoamento em duto e sua aplicação em controle de processo. Tese de Doutorado, UFPB, João Pessoa, 2016.

SLANGEN, R. A. C. M. Experimental investigation of artificial boundary layer transition. [s.l.] Delft University Technology, 2009.

SUVASH C. Saha, M.M.K. Khan, Y.T. Gu. Unsteady buoyancy driven flows and heat transfer through coupled thermal boundary layers in a partitioned triangular enclosure. International Journal of Heat and Mass Transfer, v. 68, p. 375-382, 2014.

THOMAS, Lindon. A Simple Integral Approach to Turbulent Thermal Boundary Layer Flow. Journal of Heat Transfer, v.100, n. 4, p 744-746, 1978.

8. RESPONSIBILITY NOTICE

The author(s) is (are) the only responsible for the printed material included in this paper.